Weak boundary treatment for high order transient analysis of MTLs

Weak Boundary Treatment for High-Order Transient Analysis of MTL's

S. Grivet-Talocia
Dip. Elettronica, Politecnico di Torino
Corso Duca degli Abruzzi 24
I-10129, Torino, Italy

F. Canavero
Dip. Elettronica, Politecnico di Torino
Corso Duca degli Abruzzi 24
I-10129, Torino, Italy

Abstract: This paper presents an innovative treatment of the boundary conditions for the transient simulation of arbitrary interconnects with high-order and/or wavelet-based adaptive schemes. These can be shown to provide better accuracy and less dispersion than standard FDTD schemes. A weak treatment of the boundary conditions allows to prove explicitely the strict (late time) stability of the discretized system, while preserving high-order accuracy also at the boundaries. This procedure can be applied to the discretization and simulation of possibly complex interconnect networks with arbitrary nonlinear and/or dynamic junctions. Results are given for explicit and implicit fourth-order accurate schemes in both space and time.

INTRODUCTION

There are several techniques available in the literature for the transient simulation of arbitrary transmission-line structures. Perhaps the most commonly used for electrically long lines is the Finite-Fifference Time-Domain (FDTD) scheme [6], which is second-order-accurate in space and time. However, when the rise/fall times of the involved signals are very short, the overall simulation accuracy is affected by numerical dispersion, unless a very fine grid is used. This translates into increased memory occupation and simulation times.

Two possible strategies for the optimization of the simulation tools are to employ high-order accurate schemes or time-space adaptive schemes based, e.g., on wavelet expansions. It is even possible to combine both strategies into a fast and accurate transient solver [2]. However, the inclusion of arbitrary boundary conditions due to the presence of general circuit terminations, which can be dynamic and nonlinear, is a difficult task. In particular, enforcing high-order accuracy at the boundary nodes can seriously affect the time stability of the discretized evolution equations. This problem is well-known in the Computational Fluid Dynamics literature [9].

We overcome this problem by defining an alternative way to enforce the boundary conditions related to the termination networks. The proposed strategy is based on a weak treatment of the borders. Instead of eliminating some of the border unknowns through the boundary equations, all the unknowns related to nodal voltages and currents induced by a spatial discretization of the MTL equations are retained, including the boundary voltages and currents. The termination equations are treated separately with their own set of input voltages and currents. The connection between MTL's and terminations through Kirchhoff laws is then enforced not exactly, but with the introduction of a small boundary error. This error is properly weighted and added in a stable way to the evolution equations. The resulting additional terms act as a "numerical glue", so that the dynamics of the resulting discrete system shows a stable control of the overall approximation error with the same order of accuracy both at inner and at boundary nodes.

We first illustrate in next section the boundary conditions implementation strategy through a simple test problem consisting of a scalar lossless transmission line. The, we will detail the generalization to lossy multiconductor interconnects and to interconnects networks with arbitrary topology and arbitrary nonlinear/dynamic junctions. Finally, numerical results and validations will be provided.

SCALAR TEST EQUATION

Let us consider the scalar transmission line problem

$$\begin{cases} a_t + c\,a_z = 0, \\ b_t - c\,b_z = 0, \\ a(0,t) = \Gamma_0\, b(0,t), \\ b(\mathcal{L},t) = \Gamma_1\, a(\mathcal{L},t), \end{cases} \tag{1}$$

where $a(z,t)$, $b(z,t)$ are forward and backward power waves along the domain $z \in [0,\mathcal{L}]$, c is the propagation speed, and Γ_0 and Γ_1 are reflection coefficients not larger than one. Note that no independent sources are included in this example. They will be considered in the subsequent generalizations.

Equations (1) are discretized in space through a suitable difference operator described implicitely by two matrices $\widehat{\mathbf{P}}$, $\widehat{\mathbf{Q}}$ of size $N+1$, where $N+1$ is the number of nodes (including edges) in which the domain is partitioned. In

0-7803-5677-2/00/$10.00 ©2000 IEEE

particular,

$$\mathbf{u}_z = \widehat{\mathbf{P}}^{-1}\widehat{\mathbf{Q}}\,\mathbf{u} + \mathbf{e}, \tag{2}$$

where $\mathbf{u} = (u_0, \ldots, u_N)^T$ is the array collecting the nodal values of any function $u(z,t)$, $\mathbf{u}_z$ is the array collecting the nodal values of its first derivative $(d/dz)u(z,t)$, and $\mathbf{e}$ is the approximation error, which is of order τ

$$|\mathbf{e}| = O(h^\tau). \tag{3}$$

An explicit differentiation scheme would have $\widehat{\mathbf{P}} = I$. However, we consider the more general case of implicit schemes since the latter have been shown to be characterized by shorter differentiation stencils and better accuracy [5]. Of course, the schemes are efficient if both matrices have their nonzero elements concentrated in a very small bandwidth centered on the main diagonal. We additionally require that $\widehat{\mathbf{P}}$ is symmetric and strictly positive definite, while $\widehat{\mathbf{Q}}$ is almost antisymmetric, i.e.,

$$\mathbf{u}^T(\widehat{\mathbf{Q}} + \widehat{\mathbf{Q}}^T)\mathbf{u} = -u_0^2 + u_N^2. \tag{4}$$

Such discretization operators are said to satisfy a Summation-By-Parts (SBP) rule [8].

Let us consider the spatial discretization of the above test problem prior inclusion of boundary equations. The discrete system reads

$$\begin{cases} \widehat{\mathbf{P}}\,\mathbf{a}' + c\,\widehat{\mathbf{Q}}\,\mathbf{a} &= 0 \\ \widehat{\mathbf{P}}\,\mathbf{b}' - c\,\widehat{\mathbf{Q}}\,\mathbf{b} &= 0. \end{cases}, \tag{5}$$

where the prime indicates time differentiation, $\mathbf{a} = (a_0(t), \ldots, a_N(t))^T$ is the array collecting the nodal values of the forward power wave, and similarly for $\mathbf{b}$. If we left multiply the two equations by $\mathbf{a}^T$ and $\mathbf{b}^T$ and add the two resulting equations, we get

$$\frac{d}{dt}E(t) = -\{b_0^2(t) - a_0^2(t)\} - \{a_N^2(t) - b_N^2(t)\}, \tag{6}$$

where we have defined a total discrete energy as

$$E(t) = \frac{1}{c}\mathbf{a}(t)^T\widehat{\mathbf{P}}\,\mathbf{a}(t) + \frac{1}{c}\mathbf{b}(t)^T\widehat{\mathbf{P}}\,\mathbf{b}(t). \tag{7}$$

Note that Eq. (6) does not guarantee that the discrete energy is bounded, since the termination equations have not yet been used. Next paragraph shows how the boundary conditions can be combined with Eq. (5) insuring a nonpositive rate of change of $E(t)$ or, in other words, that the discretization is strictly stable.

We start from Eq. (6). The energy will be nonincreasing in time if we manage to add to the right-hand side proper terms that make each curly bracket nonnegative. A correct way to accomplish this when including the boundary conditions is to slightly modify the discretized system (5) by adding two so-called Simultaneous Approximation Terms (SAT) of the form [1]

$$\begin{cases} \widehat{\mathbf{P}}\,\mathbf{a}' + c\,\widehat{\mathbf{Q}}\,\mathbf{a} &= -\frac{\omega}{2}c\,\mathbf{e}_0\,\{a_0 - \Gamma_0 b_0\}, \\ \widehat{\mathbf{P}}\,\mathbf{b}' - c\,\widehat{\mathbf{Q}}\,\mathbf{b} &= -\frac{\omega}{2}c\,\mathbf{e}_N\,\{b_N - \Gamma_1 a_N\}, \end{cases} \tag{8}$$

where ω is a free parameter to be determined and

$$\mathbf{e}_0 = (1,\ 0, \cdots, 0)^T, \qquad \mathbf{e}_N = (0, \cdots, 0,\ 1)^T. \tag{9}$$

The SAT terms act as penalty parameters that weight the approximation error at the boundaries (the two curly brackets in the right-hand side terms). It can be easily shown that the above procedure leads to a uniformly fourth-order scheme, including the boundaries. The complete proof can be found in [1] and is not reported here. The rate of change of the discrete energy $E(t)$ becomes

$$\begin{aligned} \frac{d}{dt}E(t) &= -\{(\omega-1)a_0^2 + b_0^2 - \omega a_0\Gamma_0 b_0\} \\ &\quad -\{(\omega-1)b_N^2 + a_N^2 - \omega b_N\Gamma_1 a_N\}. \end{aligned}$$

The key to prove stability is to show that there exist a nonvanishing range of ω so that each curly bracket is nonnegative for any passive termination, i.e., $|\Gamma_{0,1}| \leq 1$, and for an arbitrary value of $a_{0,N}$ and $b_{0,N}$. On one hand, we must require $\omega \geq 1$. In addition, it is easy to show that positivity in insured when

$$\omega^2\Gamma_{0,1}^2 \leq 4(\omega - 1), \tag{10}$$

or, equivalently,

$$\frac{2 - 2\sqrt{1-\Gamma_{0,1}^2}}{\Gamma_{0,1}^2} \leq \omega \leq \frac{2 + 2\sqrt{1-\Gamma_{0,1}^2}}{\Gamma_{0,1}^2}. \tag{11}$$

As we are seeking for a stable discretization for any allowed value of reflection coefficients, as long as they represent passive networks, we set $|\Gamma_{0,1}| = 1$ in the above expressions. This requires

$$\omega = 2. \tag{12}$$

A few remarks are in order about the boundary conditions implementation herewith described. It should be noted that all the nodal unknowns are still present in the discretized system (8). Indeed, a conventional strong boundary implementation would have required the direct elimination of the unknowns a_0 and b_N (i.e., the reflected waves from the terminations) from the system, together with the two related border equations. As a matter of fact, it can be immediately seen from Eq.(8) that the terms proportional to ω would vanish if boundary conditions were locally enforced. The presence of the additional terms in the discretization allows to account for the boundary conditions in a weak form, by leaving the possibility that an error of order τ occur at the boundaries. The terms proportional to ω act as penalty factors in the discrete equations, weighting the approximation error in the boundary treatment and adding it in a stable way to the evolution equations. This procedure seems more appropriate for hyperbolic systems, since it is quite reasonable to admit errors of the same order at any point in the computational domain, including boundaries. Any local error is indeed advected through the entire computational domain regardless where it is generated. This additional flexibility has the remarkable advantage that strict time-stability can be proved without difficulty.

We generalize now the test problem to the case of nonlinear and dynamic terminations. To this end, we replace

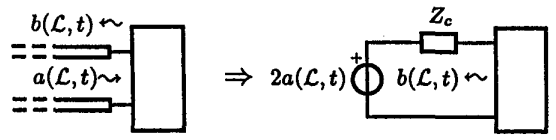

Figure 1: Equivalent circuit for the derivation of the state equations of the right termination network.

the characterization of the right-hand side termination in Eq. (1) provided by the reflection coefficient Γ_1 with the more general nonlinear state equations

$$\begin{cases} \mathbf{J}\mathbf{x}'(t) &= \mathcal{F}(\mathbf{x}(t), a(\mathcal{L},t), \mathbf{s}(t)), \\ b(\mathcal{L},t) &= \mathcal{G}(\mathbf{x}(t), a(\mathcal{L},t), \mathbf{s}(t)), \end{cases} \tag{13}$$

where $\mathbf{J}$ is a positive definite matrix, $\mathbf{x}$ is a state-variable vector related to the branch voltages and currents of capacitors and inductors in the termination circuit, and $\mathbf{s}(t)$ is an array collecting the independent sources. These state equations refer to the circuit depicted in Fig. 1, where the line is replaced by an equivalent insuring that the incident wave is $a(\mathcal{L},t)$. The series impedance Z_c is the characteristic impedance of the line, used in the definition of the scattering waves a and b. It should be noted that the dynamic behavior of the termination is forced by its internal sources and by the incident wave, while the reflected wave $b(\mathcal{L},t)$ is an output variable uniquely determined once the state $\mathbf{x}(t)$ is known.

It is instructive to compute the global energy $\mathcal{E}(t)$ stored in the system at time t. This can be computed by adding the energy stored in the transmission line to the energy stored in the termination network,

$$\mathcal{E}(t) = \frac{||a(\cdot,t)||^2}{c} + \frac{||a(\cdot,t)||^2}{c} + \frac{1}{2}\mathbf{x}(t)^T\mathbf{J}\,\mathbf{x}(t). \tag{14}$$

Its rate of change can be easily determined through time differentiation, obtaining

$$\begin{aligned} \frac{d}{dt}\mathcal{E}(t) &= -\{1-\Gamma_0^2\}\, b(0,t) \\ &\quad + [\mathcal{G}(\mathbf{x}(t), a(1,t), \mathbf{s}(t))]^2 - [a(\mathcal{L},t)]^2 \\ &\quad + \mathbf{x}(t)^T \cdot \mathcal{F}(\mathbf{x}(t), a(1,t), \mathbf{s}(t)). \end{aligned} \tag{15}$$

The evolution equations for the discretized system must account for the dynamics of the termination network. Therefore, we simply include the state equations within the weak boundary treatment framework, obtaining

$$\begin{cases} \widehat{\mathbf{P}}\,\mathbf{a}' + c\,\widehat{\mathbf{Q}}\,\mathbf{a} &= -\frac{\omega}{2} c\,\mathbf{e}_0\,\{a_0 - \Gamma_0 b_0\}, \\ \widehat{\mathbf{P}}\,\mathbf{b}' - c\,\widehat{\mathbf{Q}}\,\mathbf{b} &= -\frac{\omega}{2} c\,\mathbf{e}_N\,\{b_N - \widehat{b}\}, \\ \mathbf{J}\mathbf{x}' &= \mathcal{F}(\mathbf{x}, a_N, \mathbf{s}), \\ \widehat{b} &= \mathcal{G}(\mathbf{x}, a_N, \mathbf{s}). \end{cases} \tag{16}$$

Computation of the rate of change of the discrete energy $E(t)$, now defined as

$$E(t) = \frac{1}{c}\mathbf{a}(t)^T\widehat{\mathbf{P}}\,\mathbf{a}(t) + \frac{1}{c}\mathbf{b}(t)^T\widehat{\mathbf{P}}\,\mathbf{b}(t) + \frac{1}{2}\mathbf{x}(t)^T\mathbf{J}\,\mathbf{x}(t), \tag{17}$$

results in

$$\begin{aligned} \frac{d}{dt}E(t) &= -\{(\omega-1)a_0^2 + b_0^2 - \omega a_0\Gamma_0 b_0\} \\ &\quad - \{(\omega-1)b_N^2 + a_N^2 - \omega b_N\,\mathcal{G}(\mathbf{x}, a_N, \mathbf{s})\} \\ &\quad + \mathbf{x}^T \cdot \mathcal{F}(\mathbf{x}, a_N, \mathbf{s}). \end{aligned} \tag{18}$$

The above expressions for the continuous and discrete energy decay rates allow to derive the basic result

$$\frac{d}{dt}\mathcal{E}(t) \le 0 \quad \Rightarrow \quad \frac{d}{dt}E(t) \le 0. \tag{19}$$

In other words, any stable termination network (characterized by bounded energy when connected to a lossless transmission line) can be treated with the proposed discretization scheme, which will consequently result stable. A closer look allows to derive the following expression (only the terms referring to the right termination are reported)

$$\frac{d}{dt}\mathcal{E}(t) - \frac{d}{dt}E(t) = [b_N(t) - \mathcal{G}(\mathbf{x}(t), a_N(t), \mathbf{s}(t))]^2, \tag{20}$$

stating then the energy dissipation rate of the discrete system is exactely the same as for the continuous system anytime the boundary error (i.e., the bracketed term) is vanishing. Conversely, if a boundary error occurs, the dynamics of the discrete scheme tend to kill it through numerical dissipation.

THE GENERAL CASE

This section details the discretization process for the general lossy multiconductor case in presence of nonlinear and dynamic terminations. We consider the case of P conductors (plus reference), and state the MTL equations in compact form as

$$\frac{\partial}{\partial t}\mathbf{w} + \mathbf{\Lambda}\frac{\partial}{\partial z}\mathbf{w} + \mathbf{B}\mathbf{w} = 0, \tag{21}$$

where $\mathbf{w}$ is a column vector of size $2P$ collecting the P forward waves $a^{(i)}(z,t)$ and the P backward waves $b^{(i)}(z,t)$, $\mathbf{B}$ is a positive semidefinite matrix related to distributed losses along the line, and

$$\mathbf{\Lambda} = \begin{pmatrix} \mathbf{c} & \mathbf{0} \\ \mathbf{0} & -\mathbf{c} \end{pmatrix} \tag{22}$$

where $\mathbf{c}$ is the diagonal matrix with the propagation velocities of the various independent modes of the line. This paper deals only with DC losses. The treatment of frequency-dependent losses due to skin effect in the line conductors can be included in the proposed scheme through standard procedures such as recursive convolutions. This generalization will be presented elsewhere. The nonlinear dynamic termination networks are characterized by their state equations. For instance, the right termination is characterized by the same expressions in Eq. (13), with the incident and reflected scalar waves replaced by their vector-valued counterpart.

The formulation of the discretization scheme is given here in compact form using the Kronecker matrix product, de-

noted with the symbol $\otimes$. We recall its definition for two arbitrary matrices C (of size p, q) and D,

$$C \otimes D = \begin{pmatrix} c_{11}D & \cdots & c_{1q}D \\ \vdots & & \vdots \\ c_{p1}D & \cdots & c_{pq}D \end{pmatrix}. \quad (23)$$

The scheme reads

$$\begin{aligned} &\frac{d}{dt}\overline{\mathbf{y}} + (\mathbf{\Lambda} \otimes \widehat{\mathbf{P}}^{-1}\widehat{\mathbf{Q}})\,\overline{\mathbf{y}} + (\mathbf{B} \otimes I)\,\overline{\mathbf{y}} \\ &\quad = -\frac{\omega}{2}\begin{pmatrix} \mathbf{c}\,\mathbf{\Xi}_0 \\ \mathbf{0} \end{pmatrix} \otimes (\widehat{\mathbf{P}}^{-1}\mathbf{e}_0) \quad (24) \\ &\qquad -\frac{\omega}{2}\begin{pmatrix} \mathbf{0} \\ \mathbf{c}\,\mathbf{\Xi}_N \end{pmatrix} \otimes (\widehat{\mathbf{P}}^{-1}\mathbf{e}_N), \end{aligned}$$

where the vector $\overline{\mathbf{y}}$ collects all the $N+1$ nodal values of the $2P$ forward and backward waves, and $\mathbf{\Xi}_0$, $\mathbf{\Xi}_N$ are the vector-valued approximation errors at the boundaries. More precisely, for the left termination we have

$$\begin{cases} \mathbf{J}_0\mathbf{x}_0'(t) &= \mathcal{F}_0(\mathbf{x}_0(t), \mathbf{b}_0(t), \mathbf{s}_0(t)), \\ \mathbf{\Xi}_0 &= \mathbf{a}_0(t) - \mathcal{G}_0(\mathbf{x}_0(t), \mathbf{b}_0(t), \mathbf{s}_0(t)), \end{cases} \quad (25)$$

and for the right termination we have

$$\begin{cases} \mathbf{J}_N\mathbf{x}_N'(t) &= \mathcal{F}_N(\mathbf{x}_N(t), \mathbf{a}_N(t), \mathbf{s}_N(t)), \\ \mathbf{\Xi}_N &= \mathbf{b}_N(t) - \mathcal{G}_N(\mathbf{x}_N(t), \mathbf{a}_N(t), \mathbf{s}_N(t)). \end{cases} \quad (26)$$

It should be noted that the same formulation can be particularized to the linear dynamic termination case by expressing the nonlinear functions $\mathcal{F}_{0,N}$ and $\mathcal{G}_{0,N}$ as linear combination of their arguments through suitable matrix coefficients. The linear/nonlinear static termination case is recovered by considering only the output equations in Eqs. (25)-(26) and setting the dimension of the state vectors $\mathbf{x}_{0,N}$ to zero.

The consistency and strict stability proofs of the above scheme is not reported here but follows the same guidelines as for the scalar case. We can conclude that any multiconductor interconnect loaded with arbitrary passive and possibly nonlinear and dynamic terminations is discretized by the proposed scheme in a stable way preserving a uniform order of accuracy throughout the entire computational domain.

We give some final remarks on the treatment of interconnect networks with arbitrary junctions. We do not detail here the complete formulation in order to avoid heavy notations. However, it should be obvious that treatment of interconnect networks does not represent a more difficult problem with respect to the single multiconductor line (or *tube*). It is in fact possible to collect all unknowns related to the various tubes into a single vector. The discretized system equations will have the same structure as Eq. (24). If the tubes do not interact with each other, the resulting system matrices will be block-diagonal, with a single block corresponding to a single tube. Similarly, all junctions equations can be collected into a single global termination state system with the same structure of Eqs. (25)-(26).

TIME DISCRETIZATION

The above sections described how the spatial discretization can be performed for general interconnect structures in a stable and accurate way. We discuss here the problem of time discretization in some detail. We will show that the widely-used Leapfrog (LF) scheme based on centered second-order staggered finite differences in time could be not the best choice in conjunction with the high-order spatial discretization schemes.

There are a number of drawbacks in using LF or other second-order schemes in conjunction with spatial discretizations of higher approximation order τ. If LF is used in the time domain, the resulting truncation errors will behave as $O(\Delta z^\tau, \Delta t^2)$, where Δz and Δt are the space and time grid sizes. Therefore, the overall truncation error will be dominated by the time discretization, unless a very small step is used at increased computational cost. An optimized scheme would use the same accuracy for both space and time discretization. For this reason, we consider the fourth-order RK4 scheme as a preferrable choice for time discretization, although it has gained little attention in Computational Electromagnetics. The key advantages of RK4 are the following. First of all, it is an explicit scheme. Second, it has a quite large stability region [3], resulting in possibly larger time steps with respect to those allowed by, e.g., FDTD algorithms. Third, it can be coded quite efficiently with respect to other high-order methods. Fourth, it is a dissipative scheme that dims the poorly resolved wavenumbers. The latter property is usually regarded as a drawback in Computational Electromagnetics. However, the dissipation rate is significant only for those spatial modes that propagate at the wrong speed due to numerical dispersion [4].

The above considerations are best illustrated by the following numerical test. A fourth-order implicit scheme with LF and RK4 time stepping is applied to the test problem $a_t + a_z = 0$ on $[0, 1)$ with periodic boundaries, and initial conditions expressed by a Gaussian function centered at $z = 0.5$. The number of grid points is set to $N = 50$, and the simulation is run up to the final time $T = 40$, corresponding to 40 cyclic revolutions of the initial data. Each scheme is run at different Courant numbers $p = \Delta t/\Delta z$, within the stability range. Figure 2 shows the simulation results. It is evident from the plots that the fourth-order scheme gives far better results than the standard FDTD scheme. However, RK4 allows much larger time steps than LF at fixed accuracy. In addition, the results of RK4 are quite insensitive to the Courant number p. This is a clear advantage with respect to LF when treating transmission lines with different modal velocities, since all modes will be treated by RK4 with approximately the same accuracy. LF time stepping would be very accurate for the fast mode, being more dispersive for the slow ones.

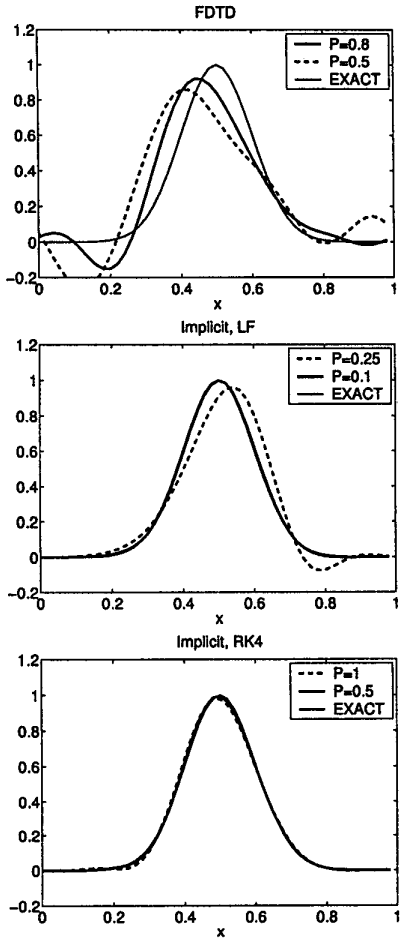

Figure 2: Accuracy of FDTD (top row), fourth-order with LF (middle row), and fourth order with RK4 (bottom row).

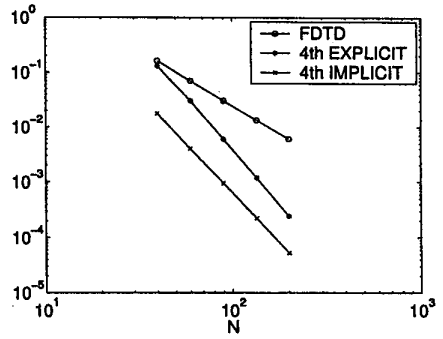

Figure 3: Comparison between FDTD and fourth-order schemes with RK4 time stepping applied to a unmatched scalar transmission line. The plot reports the L^∞ error on the termination voltage at the right boundary.

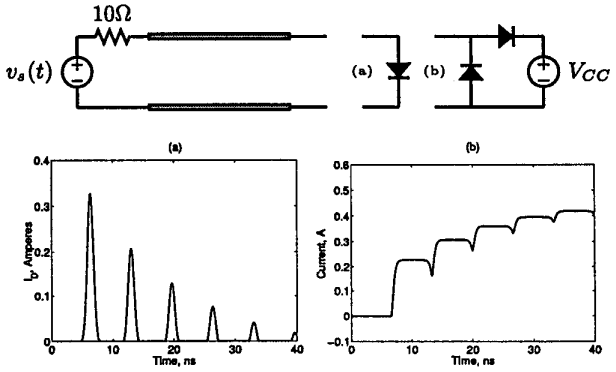

Figure 4: Currents at the right termination obtained with a fourth order scheme. Scalar line ($Z_c = 50\ \Omega$, $T_D = 3.33$ ns) loaded with a diode (a) and with a voltage protection circuit (b).

NUMERICAL RESULTS

We begin illustrating the behavior of the proposed scheme with a test case. A normalized lossless scalar transmission line (with characteristic impedance $Z_c = 1$, propagation delay time $T_D = 1$, and propagation speed $c = 1$) is excited by a gaussian series voltage source at the left termination,

$$V_S(t) = \exp\left\{-(t - T_s)^2/(2\sigma_s^2)\right\} \qquad (27)$$

with $T_s = 0.5$ and $\sigma_s = 0.08$. The series resistances of the terminations are, respectively, $R_S = 10^{-3}$, $R_L = 10^3$, i.e., $\Gamma_S = -0.998$, $\Gamma_L = 0.998$. Fig. 3 reports the maximum error at the right boundary between the exact solution and the numerical solution obtained with FDTD and with two (explicit and implicit) fourth-order schemes with RK4 time advancement. The Courant number was set in all cases to $p = 0.8$, i.e., close to the stability limit of the FDTD scheme. It is evident that the fourth order schemes perform much better than FDTD in terms of both error values and decay rate under grid refinement. It can be desumed from the plot that the achievement of a maximum error below a given threshold, say $\epsilon = 10^{-3}$, would require a very fine grid or, equivalently, a very large number of unknowns for the FDTD method (as the decay rate is N^{-2}, a simple extrapolation gives approximately $N = 700$). The same error can be obtained with the fourth-order schemes with much less grid points, about $N = 140$ for the explicit one and $N = 90$ for the implicit one.

A further example illustrates the inclusion of nonlinear terminations. The results (see Fig. 4) obtained by loading a scalar line with a shunt diode (with a 10 V Gaussian source) and with a simple voltage protection circuit (with a 10 V step source) show no difference with the SPICE simulation, also reported in the plots.

We present next the results for a more practical situation commonly encountered in the applications, a high-

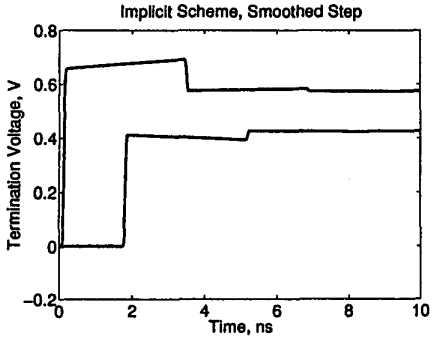

Figure 5: Termination voltages for a high-loss PCB line.

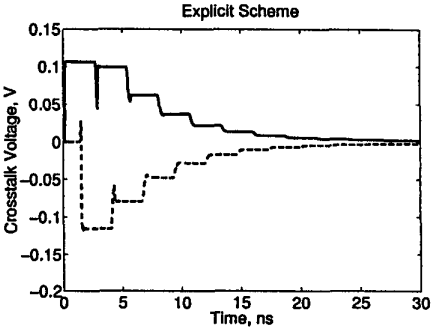

Figure 6: Near-End (continuous line) and Far-End (dashed line) crosstalk voltages for a low-loss three-conductor PCB line.

loss scalar line with a typical geometry of thin-film technology. Two PCB lands of width 20 μm and thickness 10 μm are placed on a dielectric substrate ($\varepsilon_r = 12$ and thickness 100 μm) with a separation of 20 μm. The per-unit-length parameters for this structure are (see [6], pag. 329) $L = 0.805969$ μH/m, $C = 88.2488$ pF/m, $R = 86.207$ Ω/m. The line is 20 cm long and is terminated with 50 Ω loads. A smoothed step function with expression

$$V_S(t) = \frac{1}{2} V_p \left\{ 1 + \tanh \frac{2(t - T_s - \tau_r)}{\tau_r} \right\}, \qquad (28)$$

with rise time $\tau_r = 50$ ps is applied on the left boundary, where T_s indicates the start time and V_p is the DC value of the step function. Figure 5 shows the numerical results. A total number of $N = 200$ subdivisions were used in the simulations, and the time stepping scheme was RK4 with $p = 1$.

We conclude this summary by presenting a numerical test consisting of the crosstalk analysis of a PCB structure (see [6], pp. 317 and 351). The line is made of three PCB lands placed on one side of a glass epoxy ($\varepsilon_r = 4.7$) substrate 47 mils thick. The lands have width 15 mils, thickness 1.38 mils, and their separation is 45 mils. The line is 10 inches long and is terminated with diagonal 50 Ω loads. The excitation is a step function with a rise time set to $\tau_r = 50$ ps. This very short rise time requires a fine discretization of the line. Therefore we set $N = 200$. The results are reported for a fourth-order explicit scheme in Fig. 6. There is excellent agreement with the results reported in [6].

CONCLUSIONS

A weak strategy for the implementation of boundary conditions in the discretization of multiconductor interconnects has been presented. This technique has the advantage that strict stability and uniform high-order accuracy can be rigorously proved throughout the computational domain including edges. In addition, the proposed schemes are straightforward to implement in a practical code for any type of nonlinear and dynamic termination, since no unknowns are eliminated at the boundaries. The presented numerical results and the comparisons with the standard FDTD scheme show that the proposed schemes are very promising for the reduction of the computational complexity of the currently available transient solvers for MTL structures.

REFERENCES

[1] M. H. Carpenter, D. Gottlieb, S. Abarbnel, "Time-Stable Boundary Conditions for Finite-Difference Schemes Solving Hyperbolic Systems: Methodology and Application to High-Order Compact Schemes", *J. Comput. Phys.*, vol. 111, 1994, 220–236.

[2] S. Grivet-Talocia and F. Canavero, "Wavelet-based adaptive solution for the nonuniform multiconductor transmission lines," *IEEE Microwave and Guided Wave Letters*, vol. 8, 1998, 287–289.

[3] B. Gustafsson, H. O. Kreiss, J. Oliger, *Time Dependent Problems and Difference Methods* (Wiley & Sons, NY, 1995).

[4] F. Q. Hu, M. Y. Hussaini, J. L. Manthey, Low-Dissipation and Low-Dispersion Runge-Kutta Schemes for Computational Acoustics, *J. Comput. Phys.*, vol. 124, 1996, 177-191.

[5] S. K. Lele, "Compact Finite Difference Schemes with Spectral-like Resolution" *J. Comput. Phys.*, vol. 103, 1992, 16–42.

[6] C. R. Paul, *Analysis of Multiconductor Transmission Lines*, (Wiley & Sons, NY, 1994).

[7] A. Ralston, P. Rabinowitz, *A first course in numerical analysis* (McGraw-Hill, 1982).

[8] B. Strand, "Summation by Parts for Finite Difference Approximations for d/dx", *J. Comput. Phys.*, vol. 110, 1994, 47–67.

[9] B. Strand, Numerical Studies of Hyperbolic IBVP with High-Order Difference Operators Satisfying a Summation by Parts Rule, *Appl. Num. Math.*, vol. 26, 1998, 497–521.